In situ x-ray observation of the phase transformation of Fe_2O_3

2005 J. Phys.: Condens. Matter 17 269

(http://iopscience.iop.org/0953-8984/17/2/003)

INSTITUTE OF PHYSICS PUBLISHING JOURNAL OF PHYSICS: CONDENSED MATTER

J. Phys.: Condens. Matter **17** (2005) 269–276 doi:10.1088/0953-8984/17/2/003

In situ x-ray observation of the phase transformation of Fe_2O_3

S Ono[1,4], K Funakoshi[2], Y Ohishi[2] and E Takahashi[3]

[1] Institute for Research on Earth Evolution, Japan Agency for Marine-Earth Science and Technology, 2-15 Natsushima-cho, Yokosuka-shi, Kanagawa 237-0061, Japan
[2] Japan Synchrotron Radiation Research Institute, Mikazuki-cho, Sayo-gun, Hyogo 679-5198, Japan
[3] Department of Earth and Planetary Sciences, Tokyo Institute of Technology, 2-12-1 Ookayama, Meguro, Tokyo 152-8551, Japan

E-mail: sono@jamstec.go.jp

Received 24 September 2004, in final form 23 November 2004
Published 20 December 2004
Online at stacks.iop.org/JPhysCM/17/269

Abstract

In situ observations of the phase transition in Fe_2O_3 were carried out in a multianvil and in a diamond anvil cell high-pressure apparatus using synchrotron radiation. The phase transition of haematite was observed at high pressures and high temperatures. The phase boundary between the haematite and high-pressure phase in the temperature range of 800–2500 K was determined to be P (GPa) $= 29.4(\pm 0.4) + 0.0046(\pm 0.0015) \times (T\ (\mathrm{K}) - 1000)$. This result should resolve a dispute regarding the transition pressure of haematite among previous studies on Fe_2O_3.

1. Introduction

The orthorhombic *Pbnm* perovskites, with general stoichiometry ABO_3, are derived from the ideal cubic *Pm*3*m* structure via tilting and distortion of the BO_6 octahedra [1–3]. The perovskites are of great interest in materials science because the relatively simple crystal structure displays many diverse electric, magnetic, piezoelectric, optical, catalytic, and magnetoresistive properties. In addition, perovskites are of interest in earth science because $(Mg, Fe)SiO_3$ transforms to a perovskite structure with *Pbnm* symmetry at high pressures and temperatures, and is believed to form the bulk of the Earth's lower mantle [4, 5]. In contrast, a high-pressure phase of the Rh_2O_3(II)-type structure, with general stoichiometry A_2O_3, was reported by previous theoretical and experimental studies of Al_2O_3 (e.g., [6, 7]). In the case of Fe_2O_3, the structure of the high-pressure phase is a controversial issue. Previous studies suggested two possible structures, of the perovskite and Rh_2O_3(II) types. The difference in powder diffraction pattern between them is very small. Therefore, it is difficult

[4] Author to whom any correspondence should be addressed.

to assess the structure of the high-pressure phase of Fe_2O_3 using diffraction experiments. Moreover, changes of magnetic and electronic properties, such as the electrical resistivity, spin transition, and charge-transfer, were observed in Fe_2O_3 under pressure (e.g., [8–11]). These changes are likely to be related to the crystallographic phase transition. Therefore, it is important to understand the relationship between these changes of physical properties and the crystallographic phase transition in Fe_2O_3.

Some previous high-pressure experiments suggested that the phase transition from the haematite to the high-pressure phase occurs at 50–55 GPa [10, 12–14]. In these studies, however, the phase transition was observed at room temperature. In contrast, in high-pressure and high-temperature experiments, the phase transition was observed at about 30 GPa [15, 16, 11]. If the experimental results of room temperature and high-temperature studies are both correct, this phase transition boundary has a large negative Clapeyron slope. However, kinetic effects on the phase transition were occasionally observed in room temperature compression experiments. The observed x-ray diffraction patterns reported from previous room temperature studies [12, 13] were ambiguous, because a strain broadening of the diffraction peaks occurred. It is generally known that a large differential stress is induced in diamond anvil cell experiments as pressure increases. Therefore, it is necessary to determine the phase boundary at high pressures and high temperatures.

In this study, we used a laser-heated diamond anvil cell (LHDAC) and a multianvil high-pressure system, which made it possible to acquire precise data on a sample under high-pressure and high-temperature conditions using intense x-rays from a synchrotron radiation source. Here, we report on the results of *in situ* x-ray observations of the high-pressure phases of Fe_2O_3. We also determined the phase boundary of the haematite to high-pressure phase transition in Fe_2O_3 and discuss the phase diagram of Fe_2O_3.

2. Experimental procedure

High-pressure x-ray diffraction experiments were performed using the LHDAC and the multianvil high-pressure apparatus. In the LHDAC experiments, powdered Fe_2O_3 (Wako Pure Chemical Industries, Ltd; purity 99.9%) was loaded into 100 μm holes drilled in rhenium gaskets using an excimer laser. NaCl was used as a pressure transmitting medium to reduce the diviatoric stress and temperature gradients in the sample. Gold powder was mixed with the sample to provide an internal pressure calibrant. The samples were heated with a TEM_{01}-mode Nd:YLF laser or a multimode Nd:YAG laser using double-sided laser heating techniques that minimized the temperature gradients (both axial and radial) of the heated area (figure 1). The sizes of the heating spots were about 20–30 and 50–100 μm for YLF and YAG lasers, respectively. The sample temperature was measured using the spectroradiometric method [5]. The spectroradiometric system consisted of a thermoelectrically cooled CCD detector (Princeton Instruments, HAM, 256 $\times$ 1024) and a spectrograph (Acton Research, SpectraPro-150). The temperature difference between the hot centre and cold end of the region investigated by means of x-rays in the sample was typically 150–200 K. The heated samples were probed by angle-dispersive x-ray diffraction using the synchrotron beamline BL10XU at SPring-8 in Japan [17]. The incident x-ray beam was monochromatized to a wavelength of about 0.413 Å. The x-ray beam size was collimated to 15–20 μm diameter. In order to adjust the sample position to the x-ray beam position precisely, we monitored the x-ray beam intensity distribution transmitted through the DAC by scanning the DAC stage. The shape of the sample and the gasket hole are reflected in the two-dimensional map of the transmitted x-ray intensity obtained. According to this x-ray map, we were able to set the sample on the x-ray beam position. The DAC stage itself could be controlled with the precision of 1 μm. The

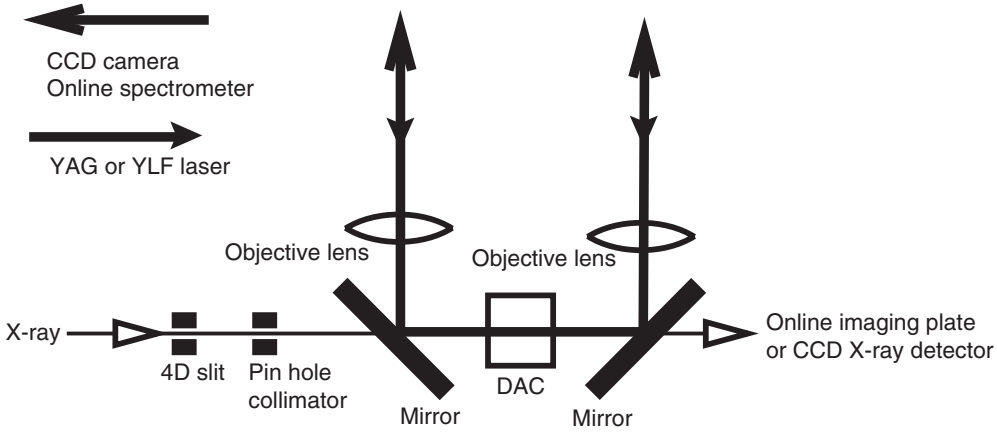

Figure 1. The *in situ* x-ray diffraction measurement system at high pressures and high temperatures combined with the laser-heated diamond anvil cell high-pressure apparatus. The system was installed at the beamline of BL10XU, SPring-8, in Japan.

sample images from both sides can be monitored by the CCD cameras through the paths of the laser optics (figure 1). During the heating, the laser beams can also be adjusted with the sample and the x-ray beam positions by the alignment of mirrors in the laser optics. Angle-dispersive x-ray diffraction patterns were obtained on an imaging plate (Rigaku) or x-ray CCD detector (Bruker). The distances between the sample and the detectors were measured using CeO_2 as a standard. The observed intensities on the imaging plates were integrated as a function of 2θ to give conventional, one-dimensional diffraction profiles. Pressure was determined from the measured unit cell volume of gold using the equation of state (EOS) for gold given by Tsuchiya [18].

The multianvil high-pressure system was composed of eight cubic anvils of sintered diamond with sides of 14 and 2.0 mm truncations [19]. The cubic anvil assembly was compressed by a high-pressure apparatus 'SPEED Mk.II' combined with a synchrotron radiation source at SPring-8 in Japan [20]. The multianvil press is a 1500 ton multianvil press equipped with an energy-dispersive x-ray diffraction system using a white x-ray at beamline BL04B1 at SPring-8. The width of both the incident and diffracted x-ray beams, controlled by adjustable slits, was 50 μm. The diffracted x-rays were detected by a germanium solid-state detector at an angle (2θ) of 5° or 5.6°. An octahedral pressure medium of Cr_2O_3-doped MgO was placed at the centre of the sintered diamond cubic anvil assembly with pyrophyllite gaskets [21]. A cylindrical rhenium heater was inserted into the octahedral pressure medium and enclosed within a $LaCrO_3$ sleeve for thermal insulation. Two carbon rods of 1 mm diameter extended from both edges of the octahedron to the rhenium heater through the pressure medium and the $LaCrO_3$ sleeve, and provided a path for incident and diffracted x-ray beams (figure 2). A powdered mixture of Fe_2O_3 and gold was prepared and used as the starting material. The powdered sample was loaded directly into the rhenium heater, which also served as a sample capsule. Sample temperatures were measured by a $W_{97}Re_3$–$W_{75}Re_{25}$ thermocouple, the junction of which was placed on the outside of the sample chamber at the centre of the furnace. No correction was made for the effect of pressure on the thermocouple emf. Pressure was determined from the measured unit cell volume of gold using the EOS for gold [18].

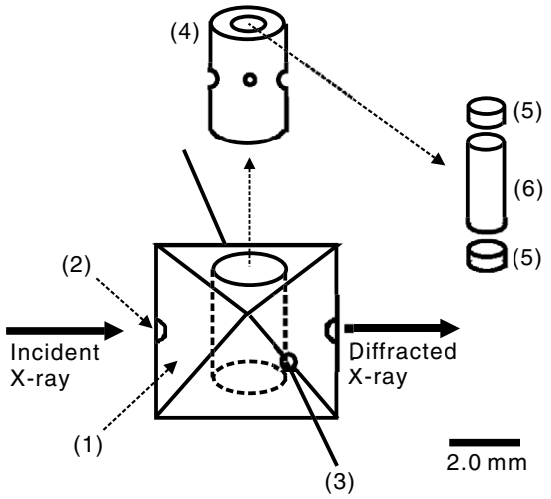

Figure 2. A schematic illustration of the cell assembly of the multianvil apparatus for high-pressure–high-temperature x-ray diffraction measurement. (1) The pressure medium of Cr-doped MgO, (2) the MgO rod, (3) the $W_{97}Re_3$–$W_{75}Re_{25}$ thermocouple, (4) the thermal insulator of cylindrical $LaCrO_3$, (5) the electrode of molybdenum, (6) the cylindrical rhenium furnace.

3. Results

In the LHDAC experiments, x-ray diffraction data were acquired at several temperatures in a heating cycle at fixed pressure loads. Heating durations were between 3 and 10 min. Typical diffraction patterns are reproduced in figure 3. Exposure times were typically between 30 and 120 s. Pressure was calculated from the EOS of gold using four diffraction lines (111, 200, 220, and 311). In the first set of LHDAC experiments, the pressure was increased directly to 15.7 GPa at room temperature, and an x-ray diffraction pattern of the sample was recorded. The diffraction pattern of the sample showed the haematite structure. This indicated that no phase transition had occurred during the compression. However, a strain broadening of the diffraction peaks occurred, resulting from the large differential stress that was induced in the diamond anvil cell experiments as pressure increased. After the desired pressure was achieved, the sample was heated to about 1450 K to relax the differential stress and to overcome potential kinetic effects on possible phase transitions. The pressure was observed to increase to 20.4 GPa as the temperature increased. This pressure increase during heating is likely to be due to thermal expansion, because the volume of the gold had nearly the same values before and during the heating. During heating, the diffraction peaks became sharp because of the release of differential stress. However, no new peaks appeared in the diffraction pattern (figure 3). This implies that the haematite structure in Fe_2O_3 is stable up to 1450 K and 20.4 GPa. After the temperature decreased to 300 K, the sample was compressed again to 24.7 GPa, and then heated. At 31.5–32.4 GPa and 1570–1880 K, the haematite structure remained stable. Moreover, the sample was compressed to 27.7 GPa after the temperature quench. When the sample was heated to 1220 K and 34.3 GPa, some new diffraction peaks appeared. These new peaks indicated that haematite transformed to the new phase at this P–T condition. When temperature increased further to 1620 K, the new phase remained stable. The crystal structure of the new phase in Fe_2O_3 has an orthorhombic symmetry. The number of formula units of this phase in a unit cell (Z) is 4. The space group of this phase is $Pbnm$ or $Pbcn$; these are generally known as the $GdFeO_3$-type perovskite and Rh_2O_3(II)-type structures. A similar

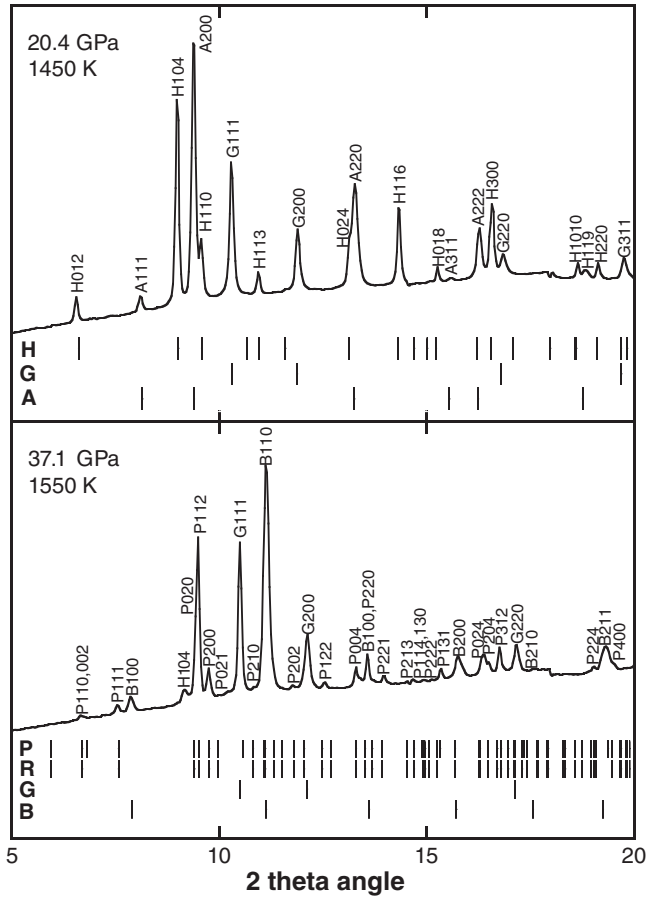

Figure 3. Examples of observed x-ray diffraction patterns of high-pressure forms of Fe_2O_3. Upper diagram: the haematite phase at 20.4 and 1450 K, $a = 4.967(1)$ Å, $c = 13.371(2)$ Å, $V = 285.74(11)$ Å^3; lower diagram: the high-pressure phase at 37.1 GPa and 1550 K, $a = 4.875(2)$ Å, $b = 5.031(3)$ Å, $c = 7.138(3)$ Å, $V = 175.07(13)$ Å^3. The abbreviations for peak labels are as follows: H, haematite; P, high-pressure phase; G, gold; A, B1-type sodium chloride; B, B2-type sodium chloride. In the bottom diagrams, vertical bars indicate the calculated positions of the diffraction lines for each phase: H, haematite ($R\bar{3}c$); P, perovskite-type phase ($Pbnm$); R, Rh_2O_3(II)-type phase ($Pbcn$); G, gold ($Fm3m$); A, B1-type sodium chloride ($Fm3m$); B, B2-type sodium chloride ($Pm3m$).

heating method was used in the other runs. We performed three runs and seven heating cycles in the LHDAC experiments. Our results for haematite and high-pressure phase stability regions are summarized in figure 4.

In the multianvil experiments, after the starting material had been loaded to the desired pressure, it was slowly heated until the stress decreased in the sample. The duration of each measurement sequence was typically 5–15 min. In the first run of the multianvil experiment, the pressure was increased to 34.0 GPa at room temperature, and the x-ray diffraction pattern of the sample was recorded. The diffraction pattern of the sample showed the haematite structure. This indicated that no phase transition had occurred during the compression. However, a strain broadening of the diffraction peaks, which was similar to that in the LHDAC experiments, was observed. While increasing the temperature, the starting material transformed to the high-

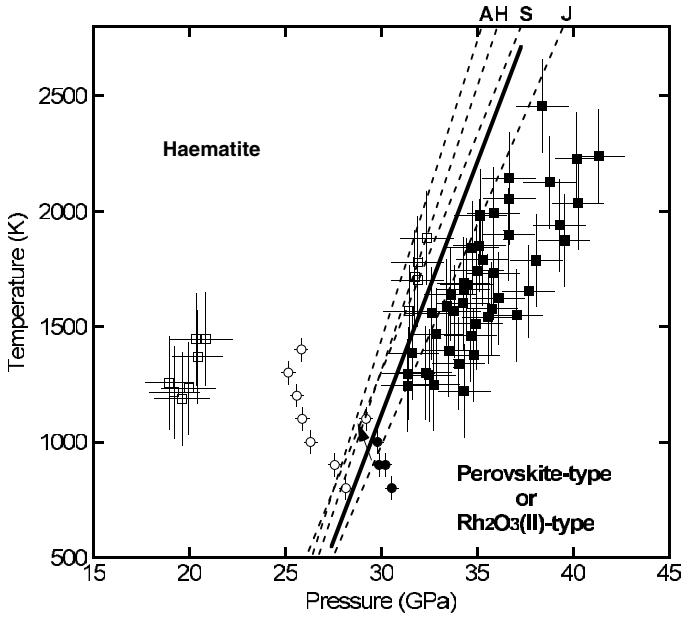

Figure 4. Experimental results and a phase boundary determined by *in situ* observation using Tsuchiya's equation of state for gold. Open squares (LHDAC) and circles (multianvil) represent conditions where haematite phases were stable, and solid squares (LHDAC) and circles (multianvil) represent the high-pressure phase. The thick line is the inferred phase boundary between haematite and high-pressure phases. An arrow indicates that the reverse transition from the high-pressure phase to haematite was observed for this condition. Dashed lines represent the phase boundaries obtained using the equations of state for gold reported from different studies: A, [25]; H, [26]; S, [24]; J, [27].

pressure phase when the temperature reached 800 K and 30.5 GPa. This indicated that the high-pressure phase was stable for this condition. When temperature increased to 1100 K and 29.2 GPa, the reverse transition from the high-pressure phase to haematite was observed (figure 4). In the second run, the pressure was increased to 24.3 GPa at room temperature and then the sample was heated. No phase transition was observed up to 1400 K and we confirmed that the haematite remained stable.

The high-temperature region was investigated by the LHDAC method because it was difficult to generalize for the region above 2000 K with the multianvil method. As the emissions from the sample cannot be observed at temperatures lower than 1200 K, the heating temperatures cannot be estimated for such low-temperature conditions in the LHDAC method. Therefore, we used the multianvil method in the low-temperature region. As the temperature gradient in the sample and the fluctuation during the heating in the multianvil method were much smaller than those for the LHDAC approach, the uncertainties of temperature and pressure were small in the multianvil method. The results of our determinations of the haematite and high-pressure phase stability regions are summarized in figure 4. The transition boundary in figure 4 is represented by the linear equation

$$P\ (\mathrm{GPa}) = 29.4(\pm 0.4) + 0.0046(\pm 0.0015) \times (T(\mathrm{K}) - 1000).$$

(Tsuchiya's equation of state for gold).

Table 1. Comparison of phase boundaries between haematite and perovskite-type phases based on different equations of state for gold. (Note: the phase boundary is represented by the linear equation P (GPa) $= A + B \times (T\ (\mathrm{K}) - 1000)$.)

References of EOS	A	B
[18]	29.4	0.0046
[24]	28.4	0.0050
[25]	28.1	0.0039
[26]	28.6	0.0041
[27]	29.9	0.0053

4. Discussion

Our results are generally consistent with previous studies [11, 15] using the heating method. However, the boundary between the haematite and high-pressure phases in this study disagrees with those determined from room temperature compression [10, 12–14]. Previous studies of room temperature experiments suggested that the phase transition occurs at about 50–55 GPa. However, the estimated transition pressure at 300 K in our study was 26.2 GPa, which is much lower than the values previously reported from room temperature studies. The pressure discrepancy between this study and room temperature compression experiments indicates that the high-temperature heating played a fundamental role in overcoming kinetic effects of the phase transition from the haematite to the perovskite structures. Another phase transition in Fe_2O_3 was reported by Ono *et al* [22]. At about 60 GPa and high temperatures, the high-pressure phase of Fe_2O_3 transforms to the $CaIrO_3$-type structure, the structure that was also observed in $MgSiO_3$ at pressures higher than 100 GPa [23]. The phase boundary between the haematite and high-pressure phases determined in this study is not inconsistent with the higher phase boundary between the high-pressure and $CaIrO_3$-type structures.

Although we used Tsuchiya's EOS for gold to determine the sample pressures, other EOSs for gold have been reported [24–27]. Other EOSs show different sample pressures for a given specific volume at high pressures and high temperatures. The discrepancies between various reference EOS values of gold sometimes produce significant effects, such as geophysical implications [28]. The difference in pressure among the EOSs for gold is about 4 GPa at 40 GPa and 2000 K. For comparison, we calculated the phase boundary using each EOS for gold in table 1 and figure 4. The calculated results indicate that using different EOSs leads to a significant change of the Clapeyron slope of the phase boundary between the haematite and high-pressure phases in Fe_2O_3.

Rozenberg *et al* [13] suggested that the high-pressure phase of Fe_2O_3 had the Rh_2O_3(II)-type structure, and observed that the volume reduction of this phase transition was about 10%. Mössbauer spectroscopy results indicated that there should be one crystallographic site for iron in the structure of the high-pressure phase [10]. As the orthorhombic perovskite structure has two different crystallographic sites, the Mössbauer results rule out the possibility of orthorhombic perovskite structure. However, the volume reduction of 3%, which was inconsistent with a previous room temperature compression study [13], was observed using the laser-heated method [16]. The discrepancy in the volume reduction is likely to indicate that the high-temperature heating played a fundamental role in overcoming kinetic effects of the phase transition from the haematite to the stable structure. The phase observed in a previous room temperature compression study may be different from that in the high-temperature heating studies. In the case of Al_2O_3, both the orthorhombic perovskite and Rh_2O_3(II)-type structures are stable at high pressures [6]. Therefore, it is important to perform further investigations on structural analysis of the high-pressure phase of Fe_2O_3 in future studies.

Acknowledgments

The authors thank Y Tatsumi, N Sata, Y Nakajima, Y Tange and T Iizuka for their help in carrying out the present work. The synchrotron radiation experiments were performed at the BL04B1 and BL10XU, SPring-8 (Proposal Nos 2002B0162-ND2-np, 2003A0013-LD2-np, 2003B0031-ND2b-np, and 2004A0017-CD2b-np).

References

[1] Glazer A M 1972 *Acta Crystallogr.* B **28** 3384
[2] Woodward P M 1997 *Acta Crystallogr.* B **52** 32
[3] Woodward P M 1997 *Acta Crystallogr.* B **53** 44
[4] Fiquet G 2001 *Z. Kristallogr.* **216** 248
[5] Ono S, Ohishi Y and Mibe K 2004 *Am. Mineral.* **89** 1480
[6] Thomson K T, Wentzcovitch R M and Bukowinski M S T 1996 *Science* **274** 1880
[7] Lin J F, Degtyareva O, Prewitt C T, Dera P, Sata N, Gregoryanz E, Mao H K and Hemley R J 2004 *Nat. Mater.* **3** 389
[8] Kondo K, Mashimo T and Sawaoka A 1980 *J. Geophys. Res.* **85** 977
[9] Knittle E and Jeanloz R 1986 *Solid State Commun.* **58** 129
[10] Pasternak M P, Rozenberg G K, Machavariani G Y, Naaman O, Taylor R D and Jeanloz R 1999 *Phys. Rev. Lett.* **82** 4663
[11] Badro J, Fiquet G, Struzhkin V V, Somayazulu M, Mao H K, Shen G and Bihan T L 2002 *Phys. Rev. Lett.* **89** 205504
[12] Olsen J S, Cousins C S G, Gerward L, Jhans H and Sheldon B J 1991 *Phys. Scr.* **43** 327
[13] Rozenberg G K, Dubrovinsky L S, Pasternak M P, Naaman O, Bihan T L and Ahuja R 2002 *Phys. Rev.* B **65** 064112
[14] Shim S H and Duffy T S 2002 *Am. Mineral.* **87** 318
[15] Ma Y, Prewitt C T, Mao H K and Hemley R J 2000 *EOS Trans. AGU* **81** S41
[16] Ono S, Kikegawa T and Ohishi Y 2004 *J. Phys. Chem. Solids* **65** 1527
[17] Ono S, Hirose K, Isshiki M, Mibe K and Saito Y 2002 *Phys. Chem. Minerals* **29** 527
[18] Tsuchiya T 2003 *J. Geophys. Res.* **108** 2462
[19] Ito E, Kubo A, Katsura T, Akaogi M and Fujita T 1998 *Geophys. Res. Lett.* **25** 821
[20] Katsura T, Funakoshi K, Kubo A, Nishiyama N, Tange Y, Sueda Y, Kubo T and Utsumi W 2004 *Phys. Earth Planet Inter.* **143/144** 497
[21] Ono S, Ito E, Katsura T, Yoneda A, Walter M J, Urakawa S, Utsumi W and Funakoshi K 2000 *Phys. Chem. Minerals* **27** 618
[22] Ono S and Ohishi Y 2004 *J. Phys. Chem. Solids* submitted
[23] Oganov A R and Ono S 2004 *Nature* **430** 445
[24] Shim S H, Duffy T S and Takemura K 2002 *Earth Planet Sci. Lett.* **203** 729
[25] Anderson O L, Isaak D G and Yamamoto S 1989 *J. Appl. Phys.* **65** 1534
[26] Heinz D L and Jeanloz R 1984 *J. Appl. Phys.* **55** 885
[27] Jamieson J C, Fritz J N and Manghnani M H 1982 *High-Pressure Research in Geophysics* (Tokyo: Centre for Academic Publishing) p 27
[28] Ono S, Katsura T, Ito E, Kanzaki M, Yoneda A, Walter M J, Urakawa S, Utsumi W and Funakoshi K 2001 *Geophys. Res. Lett.* **28** 835